Available online at www.sciencedirect.com

ScienceDirect

IFAC PapersOnLine 54-1 (2021) 767–772

Machine-Learning Digital Twin of Overlay Metal Deposition for Distortion Control of Panel Structures

Mahyar Asadi*, Michael Fernandez*, Majid Tanbakuei Kashani*, Mathew Smith*

**Applus⁺- SKC Engineering, 19165 94 Ave Surrey BC Canada*
(Corresponding Author and Presenter: mahyar.asadi@applusrtd.com)

Abstract: Cyber-manufacturing relies on smart digital-twins of manufacturing processes that can quickly act for making a wise decision. However, the cognitive computing part of the digital-twin becomes time-intensive beyond the requirement of a smart system when it uses simulation tools that solve governing constitutive equations in the form of partial differential equations (PDE). On the other hand, many artificial intelligence (AI) and machine learning (ML) solutions rely on a large data set that does not exist in many manufacturing systems. We build a hybrid digital-twin that takes advantage of an ML-based digital-twin for quick response while gaining fidelity through adaptive learning with a PDE-based digital-twin. We use our hybrid digital-twin for active exploration of various overlay metal deposition patterns in real-time. This tool enables engineers to explore and compare many patterns they need to assess metal deposition scenarios with no delay for computational time.

Keywords: cyber-manufacturing, digital twin, machine learning, metal deposition, overlay pattern, distortion control, adaptive learning.

NOMENCLATURE

ρ	Density	$(\mathrm{kg/m^3})$
c_p	Specific Heat	$(J/°C/Kg)$
q	Flux	(J/m^2)
k	Conductivity	$(J/°C/m)$
L	Specific Latent Heat	(J/Kq)
f	Phase Fraction Volume	(m^3)
h_c	Convection	$(J/°C/m^2)$
σ	Stress	(N/m^2)
b	Body Force	(N)
T	Local Temperature	$(°C)$
T_∞	Ambient Temperature	$(°C)$
∂T	Spatial Rate	$(-)$
$\nabla.$	Grad Operator	$(-)$
$\nabla^2.$	Divergence Operator	$(-)$
F	Deformation Gradient	$(-)$
F_{el}	Elastic Deformation	$(-)$
F_{pl}	Plastic Deformation	$(-)$
$F_{\Delta v}$	Thermal Deformation	$(-)$
Δv	Thermal Expansion	$(-)$
Q_t	Temporal State Vector	$(-)$
u_t	Temporal Control Vector	$(-)$
R^n	State Space	$(-)$
R^m	Control Space	$(-)$
γ	Space Mapping	$(-)$

1. INTRODUCTION

Industry 4.0 brings a leap forward from traditional automation to fully connected and intelligent manufacturing systems (Deloitte, 2017) by incorporating cyber-physical systems (CPS) (Bagheri, 2015). The brain of the cyber-physical system (CPS) platforms consists of cyber-twin systems that are the digital representation of physical assets. This digital twin is designed to act as the system's brain to make wise decisions through data communication with the digital muscles embedded in the physical assets (Kritzinger, et al., 2018). Constructing a digital twin (DT) can take two general forms, including data-driven DT and knowledge-driven DT (Asadi, 2020). The data-driven DT relies on extensive data availability. Therefore, it is suitable for the applications with mass productions such as automotive, electronics, and textiles to generate large data sets at a low cost (Abuali, 2020).

In contrast, the knowledge-driven DT uses the physical understanding of the processes to reduce the data required for prediction (Asadi, et al., 2019). The majority of manufacturing sectors do not have a large dataset to draw-on, and the cost of generating such a large data set is high. This data-deficiency limits the application of AI and digital twins for many manufacturing and fabrication facilities. Engineers use digitalization tools for constructing a digital twin of the physical assets (Krasnov, et al., 2019). However, digital twins that are entirely built on deploying simulation tools such as

10.1016/j.ifacol.2021.08.089

Finite element analysis (FEA) are limited by computational time for real-world applications. FEA needs solving partial differential equations (PDE) that take significantly long CPU time even on a super-computer for an industrial-scale problem. Using machine learning (ML) advantages, FEA and ML have been integrated to solve this problem, where ML algorithms emulate the behaviour of the time-consuming PDE-solver for real-time analysis of PDE in a given application (Bayat, et al., 2020). The integration of ML and FEA provides a platform for theory-training ML (Torabi Rad, et al., 2020) (also known as physics-guided ML (Willard, et al., 2020)), where one can construct a knowledge-driven digital twin using limited data rather than relying on a large dataset.

This paper builds a quick learner using a physics-guided ML approach in conjunction with an active learning strategy (Settles, et al., 2012). The fabrication process is the overlay metal deposition on panel structures. The objective is to control the distortion induced to the structure due to massive metal deposition during the overlay process. The pattern of depositing metals to cover the overlay area is an open challenge for many fabrication engineers to lower the distortion (Adak, et al., 2010). Our quick learner is now mature in predicting final overlay distortion for a given arbitrary deposition pattern. Our methodology reaches the maturity-level with less than hundreds of data labelling using FEA analysis. Many validation tests confirm that our learner can emulate the PDE-based models at reduced CPU-time from hours to seconds. The learner packages as a cloud-based tool that enables engineers to explore and compare as many as the pattern they need to assess for deciding with no delay for background computational time.

2. OVERLAY METAL DEPOSITION

Overlay metal deposition (also known as cladding or overlay welding) is widely used to restore the original dimension after in-service metal-loss locally, but coming with undesirable features such as adding significant distortion to the initial structural shape. Many procedures and machines are available to help reducing distortion; however, the pattern of depositing metals remain an open challenge for lowering the distortion. There is no optimal pattern that fits all applications. The nature of finding the best practice is case-specific based on the location, size, and surrounding constraints of structure around the overlay area. On the other hand, the variation of patterns is vast to try and find the best one. Therefore, mock-up physical testing cannot be a solution, and engineers are using digitalization tools for exploring different scenarios on a digital twin of the actual structure.

A digital twin can be defined as a control problem with a sizeable time-dependent vector "Q_t" that describes our problem's state space at the time "t" through coordinates of all geometrical points on the panel. PDE-based DT governs the state space that maps $\gamma : R^m \rightarrow R^n$, where R_m is the control space and R_n is the state space. The control vector "u" consists of two arrays of sixty-four strings each, including one array to define the given deposition pattern, and the second array defines the stiffeners. Figure 1 represents an interpretation of digital twin as a control problem with the mathematical form as in (1).

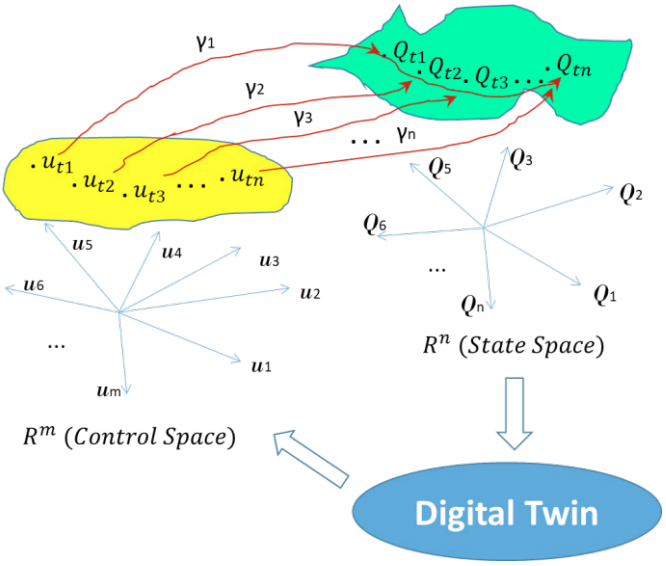

Figure 1 Digital twin as a control problem.

$$\begin{cases} R^m \rightarrow R^n \\ Q_t = \gamma\,(Q_{t-1}, u_t) \end{cases} \quad (1)$$

This mapping plays a critical role in constructing a digital twin (DT) with control of the overlay metal deposition. A quick method that can solve this mapping in a feasible time and cost enables the DT's optimization and design space exploration. PDE-driven DT, such as FEA models, can solve this mapping with high fidelity but at a high cost and long CPU time. On the other hand, data-driven DTs are quick and cheap in solving this mapping, but they need a large amount of data to gain an acceptable fidelity. Such an extensive data set does not exist in the overlay processes. Therefore we developed a hybrid DT that can maintain a balanced use of PDE-driven and data-driven methodologies to form a quick DT with reasonable fidelity for this control problem.

We use an eight-by-eight reference-grid on the overlay plate to define the user's arbitrary pattern by sixty-four chunks of metal deposition (Figure 2 top). We use a mirror of the reference-grid on the other side of the panel to define the stiffeners where chunks become fixed on stiffeners' location in the mechanical analysis (Figure 2 bottom). Figure 3 shows an example of the user's arbitrary pattern for metal deposition on the panel's DT with four passes and two crossed stiffeners underneath. There is no limitation on the user's patterns, the number of weld passes, start-stop points, the sequence of depositions, and stiffeners' location. The DT can support panels with different stiffeners' configurations, ranging from no stiffeners to parallel stiffeners and cross stiffeners.

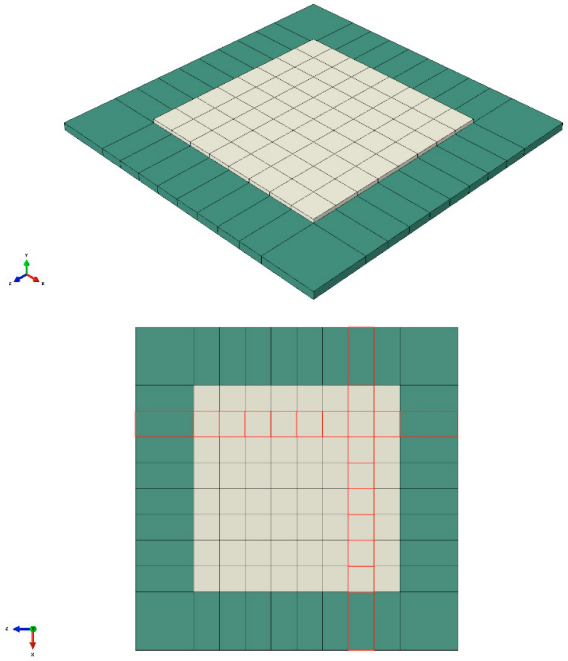

Figure 2 The eight-by-eight reference-grid on the overlay plate (top) and an example of stiffeners definition on the mirror reference-grid (bottom).

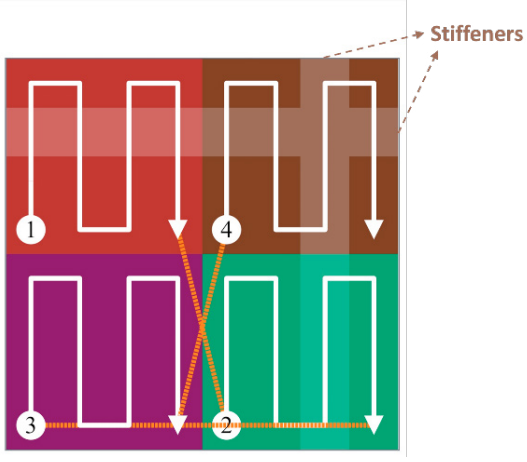

Figure 3 An arbitrary pattern of metal deposition on the panel's DT with four passes and two crossed stiffeners underneath.

3. PDE-BASED DIGITAL TWIN

We created a full 3D digital model of the overlay panel-plate using Abaqus Welding Interface (AWI) and in-house subroutines. This digital twin represents the panel's distortion for a given deposition pattern. The moving heat-source can define either as a flux-based (i.e. Neumann boundary condition) or Temperature-based (i.e. Dirichlet boundary condition) in the PDE-solve of the conservation of energy equation (Goldak, et al., 2005). We used the Dirichlet temperature because it was closer to our calibration. The 3D transient temperature is determined by solving the partial differential equation for the conservation of energy (as in (2) (Goldak, et al., 2005)) for a Lagrangian or material formulation.

$$\rho\, C_p \dot{T} + k\, \nabla^2 . T - \rho L df = 0 \qquad (2)$$

An ambient temperature of 27 °C is the initial and final temperature. A temperature-dependent convection boundary condition generates a boundary flux q (w/m^2) on all external surfaces (as in (3) (Kumar, et al., 2008)).

$$q = h_c\,(T - T_\infty) \qquad (3)$$

$$h_c = 5 + 0.05(T - T_\infty) + 6 \times 10^{-7}(T - T_\infty)^3$$

Using the eight-by-eight reference-grid (Figure 2) allows for the automation of each deposition pattern and calculates each chunk's deposition time from the torch speed. There is a final step of a cool-down model for returning thermal profile to ambient temperature at the end of the overlay process. Material properties are temperature-dependence and taken from (Valencia, et al., 2008). Figure 4 shows some snapshots of thermal analysis for the pattern in Figure 3 when depositing different each weld passes.

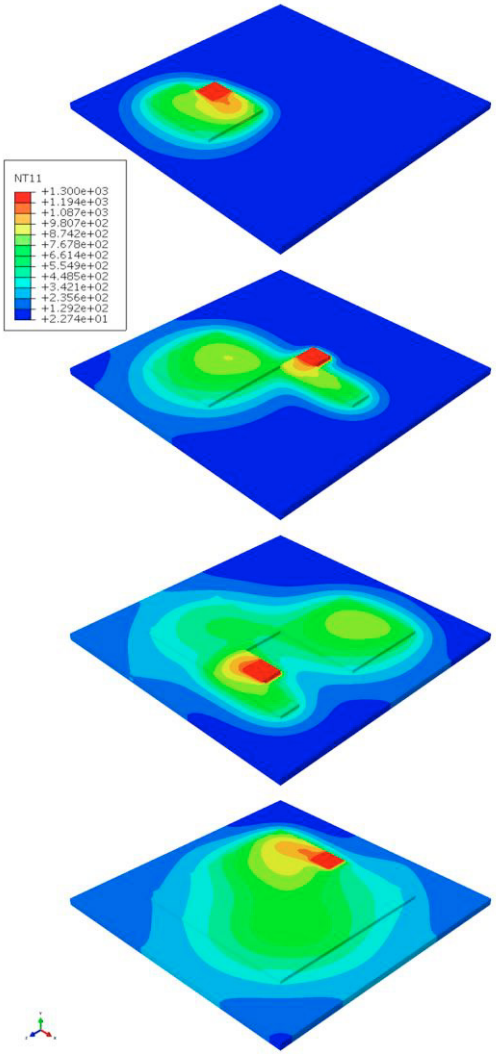

Figure 4 Snapshots of thermal analysis for the pattern in Figure 3 when depositing chunks 11, 22, 39, and 64 from top to bottom, respectively.

The stress analysis is quasi-static, and the domain is in static equilibrium in each time-step of chunk deposition because the dynamic force is sufficiently small and neglected. However, the temperature is time-dependent and therefore, the thermal strain due to thermal expansion is time-dependent. Stress analysis takes a general form of solving the virtual work statement and the conservation of equilibrium using thermo-elastic-plastic formulation (Simulia, 2014) with isotropic hardening (Simo, 1998). The deformation gradient "F" is the multiplicative decomposition of elastic deformation(F_{el}), plastic deformation(F_{pl}), and thermal expansion($F_{\Delta v}$), as in (4). Figure 5 shows the panel's distortion at the end of depositing pattern in Figure 3.

$$\begin{cases} \nabla \cdot \sigma + b = 0 \\ F = F_{el} F_{pl} F_{\Delta v} \end{cases} \tag{4}$$

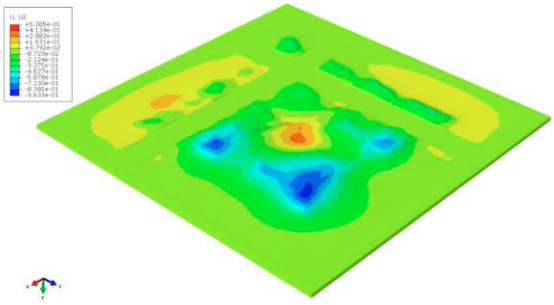

Figure 5 Panel's distortion on PDE-based DT at the end of depositing pattern in Figure 3.

4. ML-BASED DIGITAL TWIN

We borrow the eight-by-eight reference-grid from the PDE-based DT and embed it in ML-Based DT on the overlay plate to capture the user's arbitrary pattern from cursor movement on the screen. This grid converts any pattern to a unique binarized array of sixty-four strings. An identical FEA mesh characterizes the panel's distortion in our digital twins by visualizing the nodal displacements.

We build the ML-based DT using a convolutional neural network (CNN) with tremendous learning capacity. We train the CNN with the array of deposition in bi-dimensional regular patterns to predict nodal distortions on the panel's mesh (Figure 6). Physics-guided ML expedites the learning rate of a neural network towards higher fidelity. The physics of the panel's distortion shows that the distortion is lesser for a deposition closer to the edge of the panel, and it becomes significant around the panel's centroid. Therefore, we added an array of geometrical features to the CNN that includes distances between each deposition's location and the structure centroid then two closets edges (Figure 6). The stiffeners' location defines in a binary mask with a similar sixty-four grid where "1" represents the stiffeners (Figure 6).

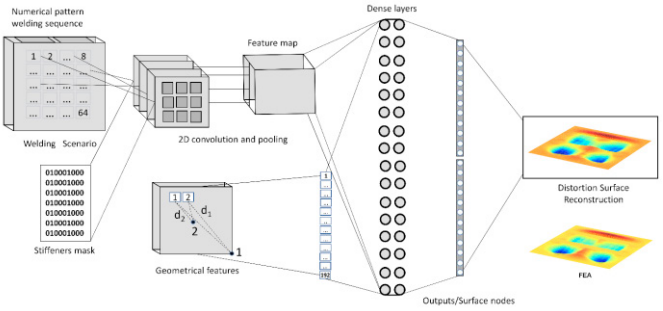

Figure 6 Schematic representation of the convolutional neural networks (CNN) used in our ML-based DT.

Five characteristic structures encompass the variation of stiffener configurations, including one with no stiffeners. We deploy the pool-based active learning using a query by committee (QBC) algorithm (Settles, et al., 2012) to train our ML-based DT with minimum labelling of the overlay deposition patterns. We use the PDE-based DT for labelling our patterns. Our active learning algorithm has identified eighty-two deposition patterns that can build-up sufficient fidelity in ML-based DT if labelled with the PDE-based DT. The PDE-based DT has labelled 410 queries (i.e. 82 patterns times five characteristic structures) for gaining 90% fidelity.

Our test set contains 50 randomly selected patterns for evaluating the model's performance. The training of the CNN model uses an early stopping strategy to mitigate overfitting. Our optimum model consists of 24 convolution layers with kernel size six connected to a pooling layer with a pooling area of three and a fully connected to a dense layer of 1,000 neurons that finally connects to the node distortion output vector. The geometrical feature vector of size 192 has also connected to the dense layer for further accuracy refinement (Figure 6).

The output of the CNN is the nodal displacements on the original mesh that characterizes the panel. Figure 7 shows the panel's distortion at the end of depositing pattern in Figure 3.

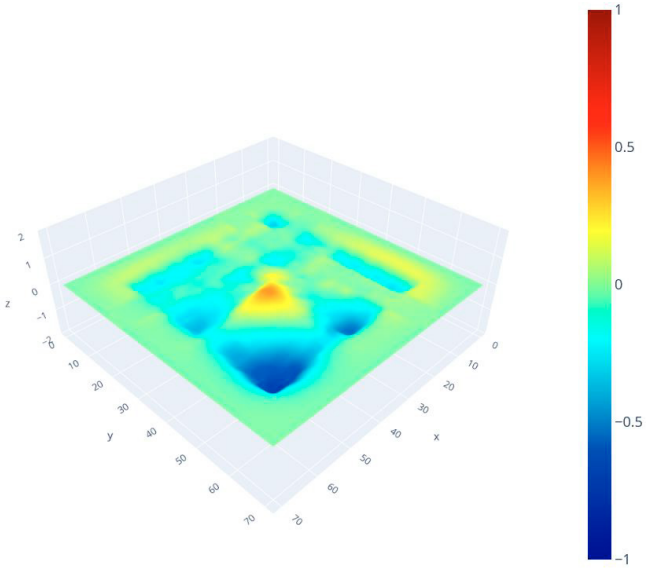

Figure 7 Panel's distortion on ML-based DT at the end of depositing pattern in Figure 3.

5. QUERY BY COMMITTEE (QBC) ALGORITHM

QBC is a disagreement-based approach for making a decision that uses a "committee" (or ensemble) with various hypotheses and a heuristic for measuring disagreement among them.

Deep learning tools do not capture the model's uncertainty; however, a recently proposed framework uses dropout training in deep neural networks (DNNs) as approximate Bayesian inference in deep Gaussian processes (Gal, et al., 2016). This method yields the uncertainty of models with dropout DNNs, and it mitigates the problem of missing uncertainty in deep learning without sacrificing either computational complexity or test.

We form various committees by dropout training in our CNN, and our QBC measures disagreement by the variance among committee members' predictions.

6. COMPARING PERFORMANCE

Our ML-based DT can instantly predict distortion with an average error of 0.8 mm for test set deposition patterns, an acceptable prediction in overlay deposition practice. Table 1 summarizes the statistical report of the performance.

Table 1 Statistical report of the ML-based DT performance

	R^2	RMSE
Training	0.983	0.043
Validation	0.909	0.083
Test	0.910	0.082

We selected three scenarios, shown in Figure 8, for evaluating the performance of our DT. The first two scenarios use different deposition-patterns on a similar stiffener's configuration, and the third scenario uses a different stiffener's configuration. Figure 9, Figure 10, and Figure 11 compare the deflection computed in PDE-based DT and ML-based DT for scenario (a), (b), and (c) in Figure 8, respectively. We include the R^2- Plots as a quantified measure of the evaluation between the two DTs. We challenged our ML-based DT with a large number of deposition scenarios to evaluate a vast performance including excellent predictions (i.e. high R^2 value) and poor predictions (i.e. low R^2 value). We have chosen Figure 8 (a) among the poor predictions with a low value. This prediction is practical for using on an overlay deposition. A set of ML-based DT scenarios with low R^2 values goes to PDE-based DT for labelling and adding to the training set.

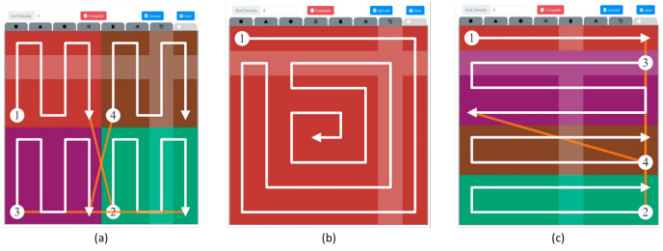

Figure 8 Three selected scenarios for evaluating the performance of our DT.

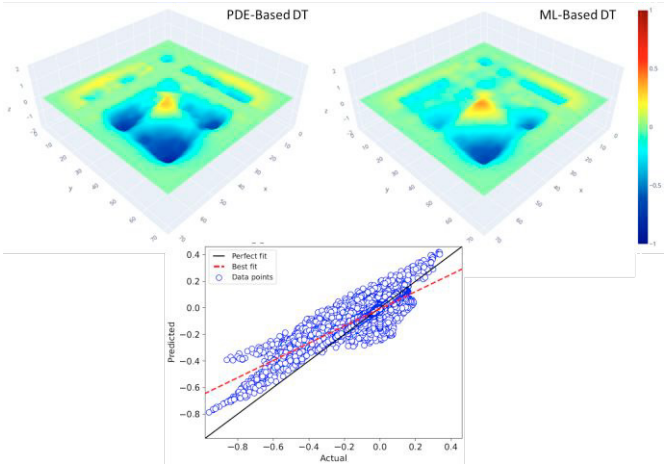

Figure 9 Comparing deflection computed in PDE-DT & ML-DT for scenario (a) in Figure 8 - R^2= 0.79.

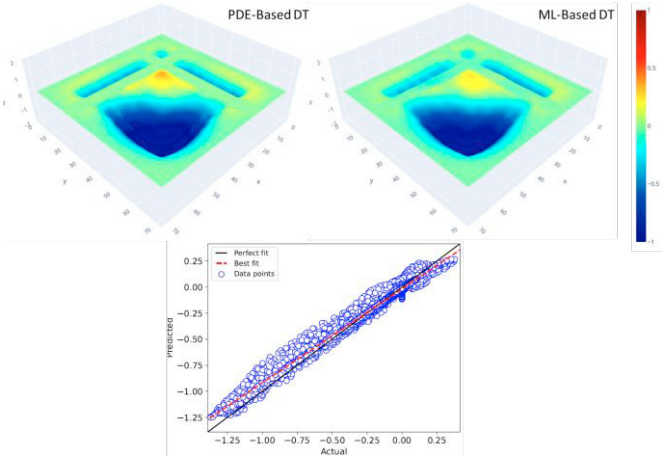

Figure 10 Comparing deflection computed in PDE-DT & ML-DT for scenario (b) in Figure 8 - R^2= 0.98.

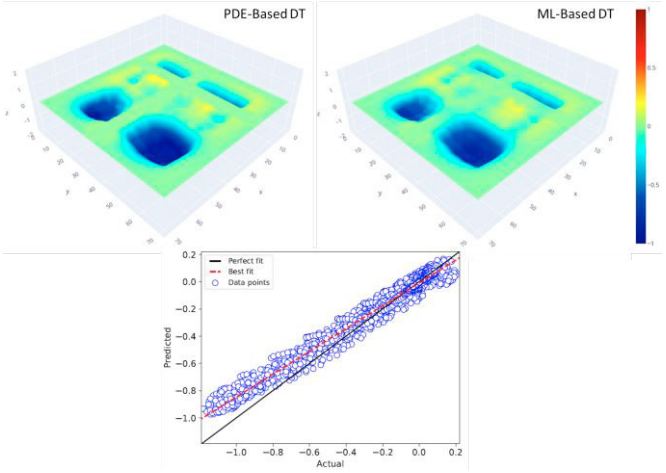

Figure 11 Comparing deflection computed in PDE-DT & ML-DT for scenario (c) in Figure 8 - R^2= 0.97.

The highlight of our ML-based DT is a significant drop in computational time. A typical computational time is about 8 hours for PDE-based DT to predict the distortion. The computational time drops to an instant response (i.e. a fraction of a second) to predict ML-based DT's distortion.

6. CONCLUSIONS

A practical DT must enable a responsive exploration of scenarios in control space. Current responsive DTs are data-driven and relies on extensive data availability. Many manufacturing sectors do not have such an extensive dataset, and the cost of generating the data is high. Therefore, they choose knowledge-driven DTs that are physics-based and use fewer data but coming with an undesirable response time. Our alternative is a hybrid DT that is responsive as data-driven DTs while gaining fidelity from knowledge-driven DTs. The hybrid DT is application-specific and needs adaptive training to select minimal data points and label them. Once we train the digital twin to reach an absolute fidelity for a given application, it becomes responsive in predicting new control vectors.

A typical data-driven DT requires several thousands of data to be capable of predicting new control vectors. Active learning methods wisely navigate data selection toward a higher training rate and gain fidelity using critical data points rather than an aggregated data set. We build a hybrid DT of overlay metal deposition for distortion control of panel structures. The control vector is an arbitrary pattern of deposition and the stiffeners configurations. The control function returns the state of distortion in the panel. This hybrid DT uses 410 inquiries for data labelling through simulation. The fidelity of distortion prediction reaches $\boldsymbol{R^2}$ value better than 0.9. Poor predictions drive the evolution of iterative training by submitting inquires for labelling to the simulation.

The response time for prediction of distortion drops from 8 hours on PDE-based DT to instant response in less than a second from ML-based DT. This hybrid DT is a responsive control tool that enables engineers to become innovative when seeking the best pattern for minimal distortion among many possibilities.

REFERENCES

Abuali Mo Artificial Intelligence in Manufacturing: Case Studies on Predictive Maintenance and Predictive Quality [Conference] // AI Manufacturing Conference. - Dallas TX - Virtual : [s.n.], 2020.

Adak M and Mandal Nr Numerical and Experimental Study of Mitigation of Welding Distortion [Journal] // Applied Mathematical Modelling. - 2010. - 1 : Vol. 34. - pp. 146-158.

Asadi Mahyar [et al.] Active Exploration of Weld Distortion Scenarios on Digital Twin [Conference] // CanWeld . - Halifax, NS : [s.n.], 2019.

Asadi Mahyar AI Challenges in Cyber Manufacturing [Conference] // AI Manufactring. - Dallas TX - Virtual : [s.n.], 2020.

Bagheri Behrad Big future for cyber-physical manufacturing systems [Report]. - Cincinati OH : University of Cincinnati, 2015.

Bayat Sharareh [et al.] Real-Time Prediction of Temperature distribution in Additive Manufacturing Processes Based on Machine Learning [Conference] // International Mechanical Engineering Congress and Exposition (IMECE). - Portland, OR : [s.n.], 2020.

Deloitte The smart factory; responsive, adaptive, connected manufacturing [Report]. - UK : Deloitte University Press, 2017.

Gal Y and Ghahremani Z Dropout as a Bayesian approximation: Representing model uncertainty in deep learning [Conference] // 33rd International Conference on Machine Learning, ICML. - New York : ICML, 2016.

Goldak John and Akhlaghi Mehdi Computational Welding Mechanics [Book]. - ISBN-10: 0-387-23287-7 : Springer, 2005.

Krasnov Fedor and Khasanov Mars Digital Twin for R&D organization: approaches and methods [Journal] // International Journal of Open Information Technologies. - 2019. - 6 : Vol. 7.

Kritzinger Werner [et al.] Digital Twin in manufacturing: A categorical literature review [Journal] // IFAC PAperOnLine. - 2018. - 11 : Vol. 51. - pp. 1016-1022.

Kumar R [et al.] Model Equation for the Convection Coefficient for Thermal Analysis of Welding Structures [Conference] // 8th International Trends in Welding Research. - Pine Mountain, Georgia : [s.n.], 2008.

Settles Burr [et al.] Active Learning [Book]. - [s.l.] : Morgan & Claypool, 2012.

Settles Burr [et al.] Active Learning (Synthesis Lectures on Artificial Intelligence and Machine Learning) [Book]. - [s.l.] : Morgan & Claypool, 2012.

Simo J C Numerical Analysis and Simulation of Plasticity [Book]. - [s.l.] : Elsevier, 1998.

Simulia Mechanical Constitutive Theories [Report]. - [s.l.] : Simulia Abaqus, 2014.

Torabi Rad M [et al.] Theory-Training Deep Neural Networks for an Alloy Solidification Benchmark Problem [Journal] // Computational Materials Science. - 2020. - Vol. 180.

Valencia Juan J and Quested Peter N Thermophysical Properties [Book Section] // ASM Handbook. - [s.l.] : ASM International, 2008.

Willard Jared [et al.] Integrating Physics-Based Modeling with Machine Learning: A Survey [Journal] // Computational Physics. - 2020. - Vol. 1.